

Montana Tech Library Digital Commons @ Montana Tech

General Engineering

Faculty Scholarship

8-22-2012

Fabrication of a Large, Ordered, Three-Dimensional Nanocup Array

Joanne C. Lo
Sandia National Labs

SoonGweon Hong
University of California - Berkeley

Richard J. Anderson
Sandia National Labs

Luke P. Lee
University of California - Berkeley

David A. Horsley
University of California - Davis

See next page for additional authors

Follow this and additional works at: http://digitalcommons.mtech.edu/gen_engr

 Part of the [Nanotechnology fabrication Commons](#)

Recommended Citation

Lo, Joanne C.; Hong, SoonGweon; Anderson, Richard J.; Lee, Luke P.; Horsley, David A.; and Skinner, Jack L., "Fabrication of a Large, Ordered, Three-Dimensional Nanocup Array" (2012). *General Engineering*. Paper 5.
http://digitalcommons.mtech.edu/gen_engr/5

This Article is brought to you for free and open access by the Faculty Scholarship at Digital Commons @ Montana Tech. It has been accepted for inclusion in General Engineering by an authorized administrator of Digital Commons @ Montana Tech. For more information, please contact ccote@mtech.edu.

Fabrication of a Large, Ordered, Three-Dimensional Nanocup Array

Abstract

Metallic nanocups provide a unique method for redirecting scattered light by creating magnetic plasmon responses at optical frequencies. Despite considerable development of nanocup fabrication processes, simultaneously achieving accurate control over the placement, orientation, and geometry of nanocups has remained a significant challenge. Here we present a technique for fabricating large, periodically ordered arrays of uniformly oriented three-dimensional gold nanocups for manipulating light at subwavelength scales. Nanoimprint lithography, soft lithography, and shadow evaporation were used to fabricate nanocups onto the tips of polydimethylsiloxane nanopillars with precise control over the shapes and optical properties of asymmetric nanocups.

Publisher's Statement

Copyright (2012). American Institute of Physics. This article may be downloaded for personal use only. Any other use requires prior permission of the authors and the American Institute of Physics. The following article appeared in *Applied Physics Letters*, and may be found [here](#) at AIP.

Authors

Joanne C. Lo, SoonGweon Hong, Richard J. Anderson, Luke P. Lee, David A. Horsley, and Jack L. Skinner

Fabrication of a large, ordered, three-dimensional nanocup array

Joanne C. Lo,^{1,2,a)} SoonGweon Hong,³ Richard J. Anderson,¹ Luke P. Lee,³
David A. Horsley,² and Jack L. Skinner¹

¹Sandia National Laboratories, 7011 East Ave., MS 9102, Livermore, California 94550, USA

²Department of Mechanical and Aeronautical Engineering, University of California, Davis, California 95616, USA

³Department of Bioengineering, University of California, Berkeley, California 94720, USA

(Received 20 June 2012; accepted 7 August 2012; published online 22 August 2012)

Metallic nanocup structures provide a unique method for redirecting scattered light by creating magnetic plasmon responses at optical frequencies. Despite considerable development of nanocup fabrication processes, simultaneously achieving accurate control over the placement, orientation, and geometry of nanocup structures has remained a significant challenge. Here we present a technique for fabricating large, periodically ordered arrays of uniformly oriented three-dimensional gold nanocup structures for manipulating light at subwavelength scales. Nanoimprint lithography, soft lithography, and shadow evaporation were used to fabricate nanocup structures onto the tips of polydimethylsiloxane nanopillars with precise control over the shapes and optical properties of asymmetric nanocup structures. © 2012 American Institute of Physics. [<http://dx.doi.org/10.1063/1.4747464>]

The ability to manipulate light at subwavelength scales is critical for plasmonic applications, such as superlenses,^{1,2} optical cloaking devices,^{3–6} and nanoantennas.^{7,8} Such optical properties have been demonstrated using patterned surfaces^{3,6} and resonance-based metamaterials.^{9–11} With the advent of more sophisticated fabrication techniques that facilitate user-control over the shapes and compositions of nanoparticles, complex plasmonic nanostructures that are asymmetrically shaped^{12–14} and/or composed of multiple materials¹⁵ have been utilized to manipulate light. Specifically, three dimensional (3D) nanocup structures—nanoparticles that consist of an asymmetric gold cap with a dielectric core—exhibit an optical response that is highly tunable in the visible and infrared regions.^{13–16} Furthermore, because the opening of the conductive cap is interrupted by a dielectric material, nanocup structures facilitate a magnetic plasmon response with magnetoinductive coupling between the cup and the incident radiation.^{16,17} This property enables nanocup structures to redirect light in the direction of the transverse axis of the cup, regardless of the incidence angle (Fig. 1).^{16,17}

Previously, the primary methods for fabricating 3D nanocup arrays involve the use of nanospheres as templates.^{16,18–20} Ideally, a large, ordered 3D nanocup array would include nanocup structures that are (i) discrete (i.e., not in contact with any other nanocup structures), (ii) arrayed with subwavelength periodicity, (iii) oriented with high consistency, and (iv) accurately constructed in terms of the desired geometry. Unfortunately, fabricating 3D nanocup arrays that satisfy these criteria has remained a significant challenge due to the use of nanospheres as templates. For example, techniques which employ self-assembled nanospheres have been used to create arrays of nanocup structures with uniform orientation and subwavelength periodicity; however, the fabricated nanocup structures are not discrete.²⁰ In contrast, while discrete, uniformly oriented nanocup structures have been fabricated using randomly spaced arrays of nanosphere templates, these nanocup arrays inher-

ently lack consistent periodicity.^{16,18,19} Additionally, for the aforementioned techniques, the shape of the nanosphere template restricts the shape of the nanocup structures. Here we overcome these challenges by instead using a large, ordered nanopillar array as a template for constructing 3D nanocup structures in order to: (i) ensure nanocup structures are discrete, (ii) tune the periodicity of the array, (iii) achieve uniform orientation of nanocup structures, and (iv) control the geometry of fabricated asymmetric nanoparticles.

To fabricate a large, ordered 3D nanocup array, Au nanocup structures were evaporated onto a periodic polydimethylsiloxane (PDMS) nanopillar array that served as a template (Fig. 2). The template was fabricated via nanoimprint lithography (NIL) (Fig. 2(a)), as described previously.²¹ The NIL template was passivated with a vapor-phase antistiction coating with Nanonex Ultra-100, and the nanofeatures were replicated using a composite stamp of hard-PDMS (h-PDMS) and soft-PDMS (s-PDMS). h-PDMS is a siloxane polymer with high Young's modulus (9 MPa) that can create high-resolution nanofeatures.²² s-PDMS, which has a Young's modulus of 3 MPa, can serve as a flexible backing for the stiff h-PDMS layer.²³ h-PDMS was prepared by first mixing 3.4 g of a vinyl

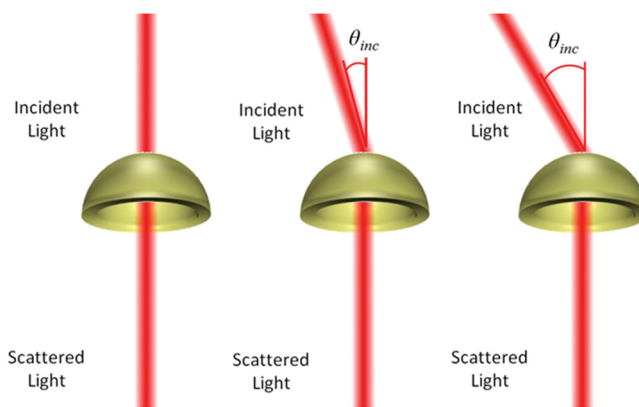


FIG. 1. Conceptual illustrations of nanocup structures redirecting light. The magnetic field enhancement within an individual nanocup structure redirects light to the direction of the nanocup axis.

^{a)} Author to whom correspondence should be addressed. Electronic mail: jlo@sandia.gov.

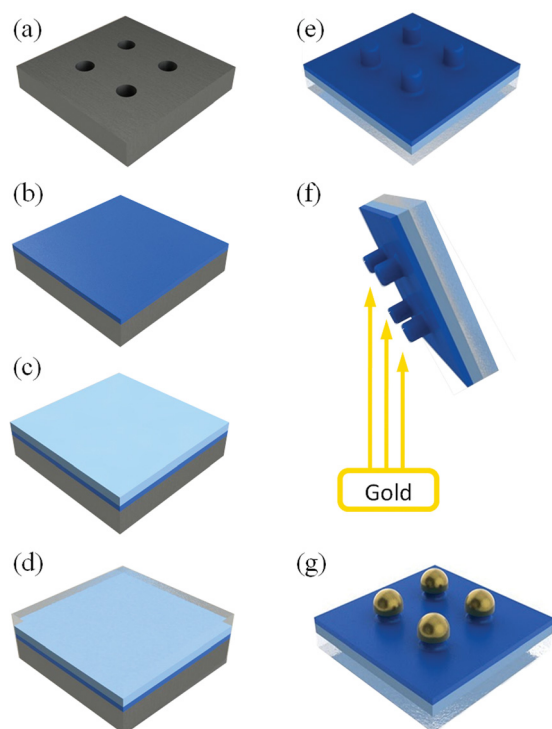


FIG. 2. Fabrication procedure. (a) A NIL template was cleaned and passivated. (b) A thin layer ($20\ \mu\text{m}$) of h-PDMS was spun onto the passivated NIL template, and partially cured at 65°C for 30 min. (c) A thick layer ($2\ \text{mm}$) of s-PDMS was poured on top of the partially cured h-PDMS. (d) A glass slide was placed on top of the s-PDMS to prevent collapse of the nanopillars. (e) The whole composite PDMS stamp was cured at 65°C for 2 h and removed after it was fully cured. (f) A thin layer of gold ($20\ \text{nm}$) was shadow evaporated onto a rotating substrate that is mounted at a 20° angle. (g) A large, ordered, nanocup array was created using the nanopillar template.

PDMS prepolymer (VDT-731, Gelest Corp.), $18\ \mu\text{l}$ of a Pt catalyst (platinum divinyltetramethyldisiloxane, SIP 6831.2, Gelest Corp), and one drop of a modulator (2,4,6,8-tetramethyltetravinylcyclotetrasiloxane, 396281, Sigma-Aldrich). After the mixture was degassed, $1\ \text{g}$ of hydrosilane prepolymer (HMS-301, Gelest Corp.) was mixed in and then the h-PDMS was degassed. The prepared h-PDMS was spun onto the passivated NIL template at $2000\ \text{rpm}$ for 30 s (Fig. 2(b)). The thin ($20\ \mu\text{m}$) h-PDMS layer was then degassed for 15 min and partially cured at 65°C for 30 min. The two-part (10:1) mixture of s-PDMS (Sylgard-184, Dow Corning) was poured onto the h-PDMS, forming a $2\ \text{mm}$ layer (Fig. 2(c)). A glass slide was then put on top of the PDMS stamp, and the whole structure was degassed for 30 min at $0.1\ \text{MPa}$ and cured for 2 h at 60°C (Fig. 2(d)). After the composite stamp was fully cured, it was separated from the NIL template (Fig. 2(e)). To create nanocup structures on the tips of the nanopillars, shadow evaporation was used to deposit a thin ($20\ \text{nm}$) layer of Au onto the nanopillar template. Shadow evaporation was performed with the nanopillar substrate mounted on a rotating plate orientated at a 20° angle (Fig. 2(f)), resulting in a large, periodic nanocup array (Fig. 2(g)). The rotating stage was designed and assembled in Sandia National Laboratories specifically for shadow evaporation. The motor attached on the bottom of the stage allowed it to rotate along its planar surface during evaporation. As the nanopillar array rotates, gold is deposited on all faces of the tip of the nanopillars, thus creating the nano-

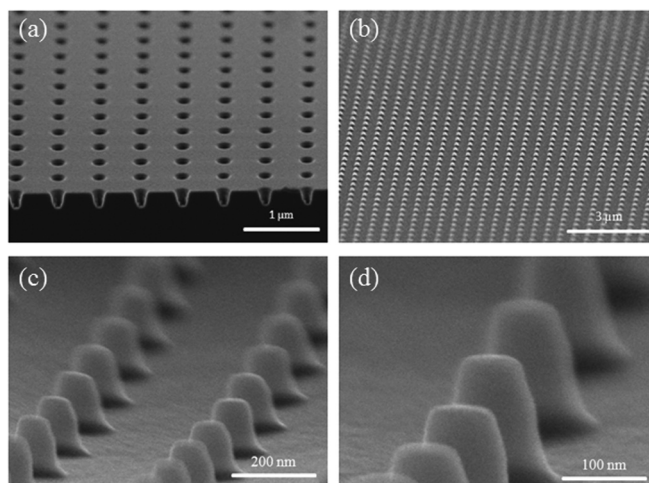


FIG. 3. SEM images of the NIL template and the nanocup array. (a) The NIL template used to fabricate the nanocup array. (b) The nanocup array, which is $0.5\ \text{cm} \times 1\ \text{cm}$ in size. (c), (d) Close-up images of the nanocup arrays. The nanocup structures are $100\ \text{nm}$ in width, $120\ \text{nm}$ in height, and $425\ \text{nm}$ in pitch.

cups. The discontinuity of the individual nanocup is not only ensured by the acute-angle deposition and the directionality of e-beam evaporation but also by the neighboring nanopillars shadowing the bottoms of the surrounding nanocup structures.

Both the NIL template and the replicated nanocup arrays were characterized with a Hitachi 4500 SEM (Fig. 3). The template and the result array were $0.5\ \text{cm} \times 1\ \text{cm}$ in size (Figs. 3(a) and 3(b)), and the nanocup structures were $100\ \text{nm}$ in diameter, $120\ \text{nm}$ in height, and $440\ \text{nm}$ in pitch (Figs. 3(c) and 3(d)). The nanocup was modeled using the software COMSOL, as a hollow gold hemisphere positioned on top of a PDMS nanopillar. The outer radius and inner radius of the nanocup were $100\ \text{nm}$ and $140\ \text{nm}$, respectively, creating a nanocup with a thickness of $20\ \text{nm}$. Two classes of simulations were performed with finite element modeling: (i) electric field enhancement, magnetic field enhancement, and extinction spectrum of a nanocup array was examined, and (ii) magnetic field enhancement of s- and p-polarizations of both a single nanocup and a $100\ \text{nm}$ symmetric gold nanoparticle were simulated with 30° angled incident light. The refractive index of h-PDMS and s-PDMS were assumed to be 1.4, and the optical property of gold was approximated with the Drude model.²⁴ The axis of the nanocup was aligned with the propagation axis of the incident wave for normal incidence, and it was placed in a medium filled with air.

The electric field and magnetic field enhancement for a nanocup array are shown in Figures 4(a) and 4(b), respectively, for a single nanocup from the array. The simulations show that at the magnetoinductive resonance frequency of $710\ \text{nm}$ (Fig. 4(c)), charge oscillations in the nanocup generate an enhanced electric and magnetic field that is symmetric with respect to the axis of the nanocup under normal incidence (Figs. 4(a) and 4(b)). The unique ability of the nanocup to redirect light is evident by comparing the magnetic field enhancement of a Au nanocup (Figs. 5(a) and 5(b)) to a solid, symmetric, $100\ \text{nm}$ gold nanoparticle (Figs. 5(c) and 5(d)) under an incident light with a 30° angle. Under an angled light incidence, the magnetic field enhancement of the nanocup remained symmetric with respect to the axis of

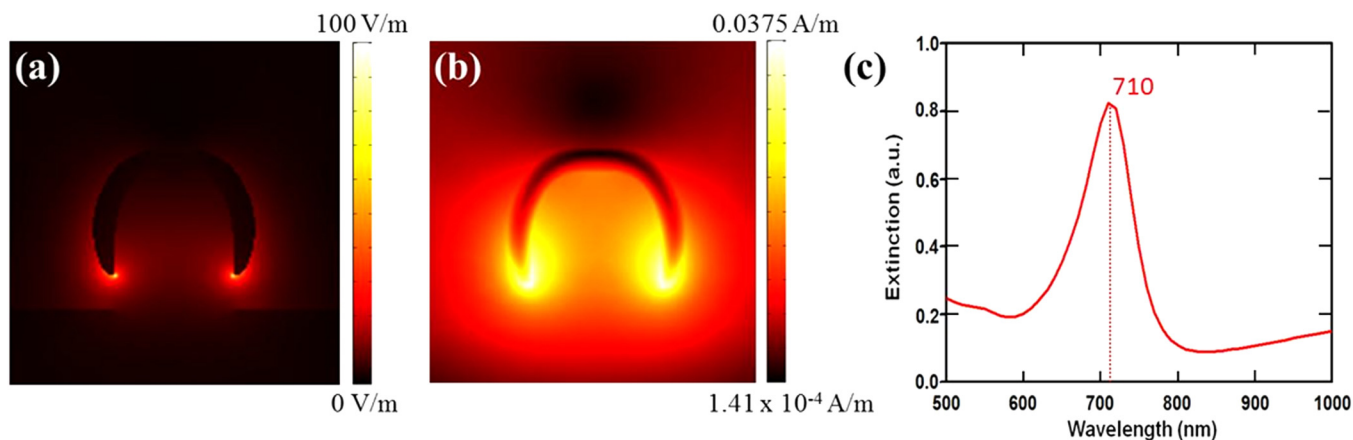


FIG. 4. COMSOL simulations of the field enhancement and optical response of the nanocup array. Simulated enhancement of the (a) electric field ($E_0 = 1$ V/m), (b) magnetic field ($H_0 = 3.67 \times 10^{-3}$ A/m), and (c) extinction spectrum.

the nanocup (Figs. 5(a) and 5(b)), whereas the magnetic field pattern of the 100-nm gold nanoparticle followed the direction of the incident light (Figs. 5(c) and 5(d)). Additionally, the magnetic field enhancement of the nanocup under angled incidence was three times greater than that of the solid gold nanoparticle (Fig. 5), demonstrating the strength of the light-redirecting magnetic field.

To observe the effect of this magnetic field enhancement on the scattered light, the nanocup array was characterized optically by measuring the extinction spectra of the array with an Ocean Optics QE65000 spectrometer with baseline subtraction. A broad-spectrum halogen light was polarized, collimated, and focused onto the sample. The optical responses of the nanocup array under s- and p-polarized light were examined. A bare PDMS slab on a glass slide was used to measure the baseline. The extinction spectra of the array were measured with different incidence angles. Generally, extinction spectra for symmetric plasmonic nanoparticles vary depending on the angle of incident light^{25–27}; however, this was not observed for nanocup arrays. Rather, the light scattering direction, and therefore the profile of the extinc-

tion spectrum, depended on the orientation of the nanocups instead of the direction of the incident light (Fig. 6).^{16–18}

The results of experimental extinction spectra show that angular independence was observed for s- and p-polarization (Fig. 6). These results demonstrate that the large, ordered nanocup array was capable of redirecting light, which indicates that the fabricated nanocups were discrete and possessed geometries that enabled charge build-up. The extinction spectra show a peak at approximately 690 nm; the position of the extinction peak and the profile of the extinction spectra remained highly similar as the nanocup rotates from 0° to 40° (Fig. 6(a)). The relatively broad linewidth observed in the optical response (Fig. 6) can be attributed to the metal thickness distribution, electron scattering at the metal interfaces, and the decrease in electron mean-free path in the nanocups.^{16,28,29} While the peak wavelength remained constant with differing angle of incidence, the magnitude of the extinction spectra varied (Fig. 6). Generally, the magnitudes of the extinction spectra for s-polarization increase with increasing incident angle (Fig. 6(a)), whereas the magnitudes of the extinction spectra for p-polarization decrease with increasing angle (Fig. 6(b)). This is because for p-polarization, the plasmonic response of each nanocup decreases with increasing angle.¹⁶ For s-polarization, the plasmonic response is isotropic for all angles.¹⁶ It can be observed that in s-polarization, the magnitude of the extinction spectrum increases at 10° (Fig. 6(a)). This increase could be attributable to the grating mode created by the periodic nanocup array.^{20,26,27} The optical response of the nanocups is red shifted (Fig. 6) compared to solid-core Au nanoparticles, which is consistent with prior studies of discrete, asymmetric nanoparticles.^{12,13,16,18–20} Since the edges of the nanocups are defined by shadowing of the neighboring nanopillars (instead of by mechanical means), the tips of the nanocups are tapered, but not ultra-sharp. This fact suggests that light-redirecting by nanocups is not caused by tip-effects, which agrees with findings from other studies on nanocups.^{16–18}

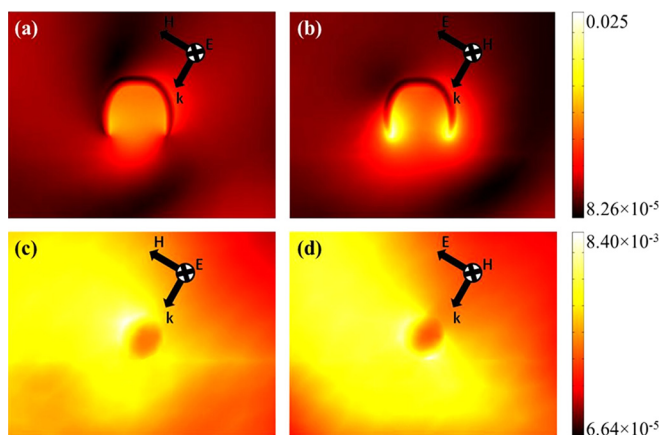


FIG. 5. Simulations of the magnetic field of a single nanocup and a 100-nm gold nanoparticle with 30° angled incident light. (a) Magnetic field enhancement of a nanocup under s-polarized angled incident light. (b) Magnetic field enhancement of a nanocup under p-polarized angled incident light. (c) Magnetic field enhancement of a gold nanoparticle under s-polarized angled incident light. (d) Magnetic field enhancement of a gold nanoparticle under p-polarized angled incident light.

Large, ordered 3D nanocup arrays provide a unique tool for redirecting scattered light at visible and near infrared wavelengths. Here we introduce a fabrication process for creating 3D nanocup arrays via nanopillar array templates to enable a high user-control over the geometry, placement,

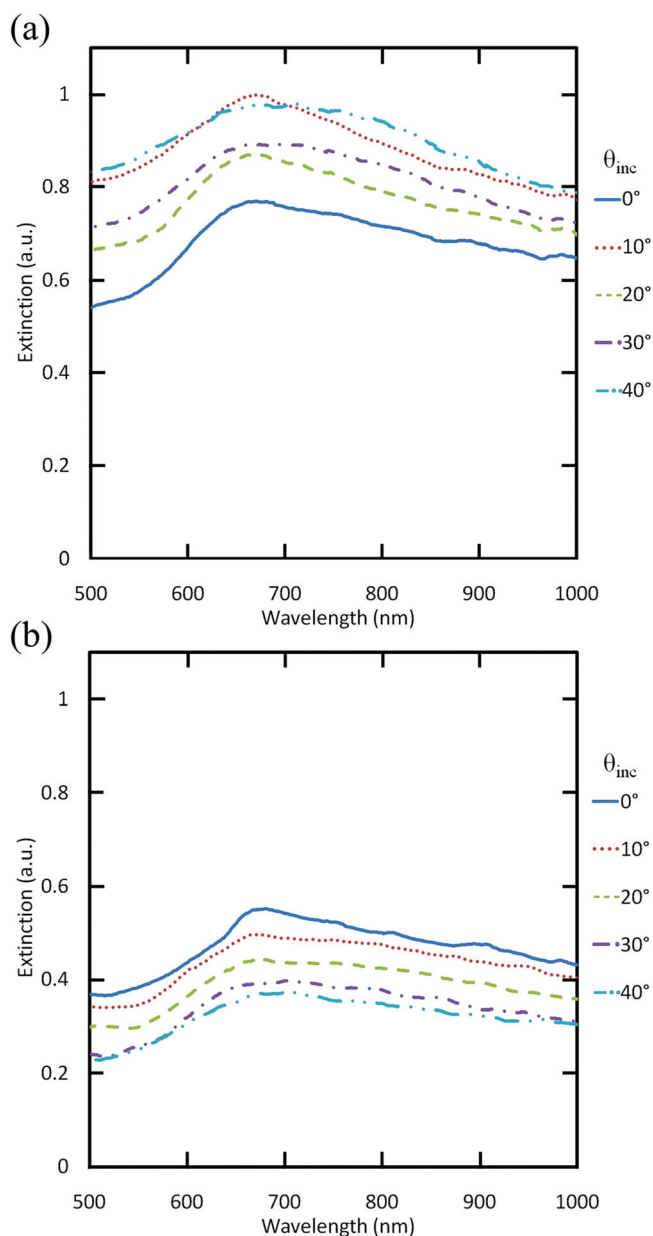


FIG. 6. Extinction spectra of the nanocup array under (a) s-polarization and (b) p-polarization. The profile exhibits angular independence while the incidence angle (θ_{inc}) is varied from 0° to 40° .

and orientation, of discrete, arrayed nanocups. Our fabrication process precludes complicated aligning, masking, and etching procedures that are frequently used for creating ordered arrays of discrete 3D nanostructures. In this study, we have demonstrated a large, ordered nanocup array that redirects light based on nanocup orientation. As asymmetric core-shell nanoparticles have highly tunable plasmonic responses, their optical response can be regulated by modifying the shapes, sizes, materials, and ratio of both the shell and the core. Additionally, this fabrication methodology can be adapted for other core-shell asymmetric nanoparticles with different geometries, bypassing limitations associated with nanosphere-based techniques. For example, nano-horseshoes can be fabricated simply by changing the tilt angle

during the evaporation process. The geometry of the nanocups can be tailored for distinct applications, including light-redirection and nanoantennas, since the strength of the current can be increased by optimizing the shape and coupling between the nanocups.³⁰ For plasmonic applications, such as superlenses, optical nanocircuits, and cloaking devices, our nanopillar-based technique offers a powerful method for fabricating large, ordered 3D nanocup arrays to manipulate light at subwavelength scales.

This work was supported by Sandia National Laboratories, California. The authors thank Charles Steinhaus, Dave Heredia, François Leonard, Ryan Sochol, Adrienne Higa, and Heather Chiamori for valuable input and proofreading of the manuscript.

- ¹X. Zhang and Z. Liu, *Nat. Mater.* **7**, 435–441 (2008).
- ²J. B. Pendry, *Phys. Rev. Lett.* **85**, 3966 (2000).
- ³J. Valentin, J. Li, T. Zentgraf, G. Bartal, and X. Zhang, *Nat. Mater.* **8**(7), 568–571 (2009).
- ⁴T. Ergin, N. Stenger, P. Brenner, J. B. Pendry, and M. Wegener, *Science* **328**, 337–339 (2010).
- ⁵U. Leonhardt and T. Tyc, *Science* **323**, 110–112 (2009).
- ⁶L. H. Gabrielli, J. Cardenas, C. B. Poitras, and M. Lipson, *Nat. Photonics* **3**, 461–463 (2009).
- ⁷P. Muhlschlegel, H. J. Eisler, O. J. F. Martin, B. Hecht, and D. W. Pohl, *Science* **308**, 1607–1609 (2005).
- ⁸S. J. Oldenburg, G. D. Hale, J. B. Jackson, and N. J. Halas, *Appl. Phys. Lett.* **75**, 1063–1065 (1999).
- ⁹N. Engheta, *Science* **317**, 1698–1702 (2007).
- ¹⁰J. Valentine, S. Zhang, T. Zentgraf, E. Ulin-Avila, D. A. Genov, G. Bartal, and X. Zhang, *Nature (London)* **455**, 376–379 (2008).
- ¹¹N. Liu, H. Guo, L. Fu, S. Kaiser, H. Schweizer, and H. Giessen, *Nat. Mater.* **7**, 31–37 (2008).
- ¹²R. Jin, Y. C. Cao, E. Hao, G. S. Metraux, G. C. Schatz, and C. A. Mirkin, *Nature (London)* **425**, 487–490 (2003).
- ¹³M. W. Knight and N. J. Halas, *New J. Phys.* **10**, 105006 (2008).
- ¹⁴E. Prodan, C. Radloff, N. J. Halas, and P. Nordlander, *Science* **302**, 419–422 (2003).
- ¹⁵R. Bardhan, S. Mukherjee, N. A. Mirin, S. D. Levit, P. Nordlander, and N. J. Halas, *J. Phys. Chem.* **114**, 7378–7383 (2010).
- ¹⁶N. A. Mirin and N. J. Halas, *Nano Lett.* **9**, 1255–1259 (2009).
- ¹⁷M. Cortie and M. Ford, *Nanotechnology* **18**, 235704 (2007).
- ¹⁸C. Charnay, A. Lee, S. Q. Man, C. E. Moran, C. Radloff, R. K. Bradley, and N. J. Halas, *J. Phys. Chem. B* **107**, 7327–7333 (2003).
- ¹⁹J. Liu, B. Cankurtaran, L. Wiecezorek, M. J. Ford, and M. Cortie, *Adv. Funct. Mater.* **16**, 1457–1461 (2006).
- ²⁰A. I. Maarouf, M. B. Cortie, N. Harris, and L. Wiecezorek, *Small* **4**, 2292–2299 (2008).
- ²¹J. L. Skinner, A. A. Talin, and D. A. Horsley, *Opt. Express* **16**, 3701–3711 (2008).
- ²²H. Schmid and B. Michel, *Macromolecules* **33**, 3042–3049 (2000).
- ²³T. W. Odom, J. C. Love, D. B. Wolfe, K. E. Paul, and G. M. Whitesides, *Langmuir* **18**, 5314–5320 (2002).
- ²⁴P. G. Etchegoin, E. C. Le Ru, and M. Meyer, *J. Chem. Phys.* **125**, 164705 (2006).
- ²⁵A. O. Pinchuk, *J. Phys. Chem. A* **113**(16), 4430–4436 (2009).
- ²⁶C. F. Bohren, D. R. Haffman, *Absorption and Scattering of Light by Small Particles* (John Wiley & Sons, New York, 1983).
- ²⁷A. Christ, T. Zentgraf, S. G. Tikhodeev, N. A. Gippius, J. Kuhl, and H. Giessen, *Phys. Rev. B* **74**, 155435 (2006).
- ²⁸S. L. Westcott, J. B. Jackson, C. Radloff, and N. J. Halas, *Phys. Rev. B* **66**, 155431 (2002).
- ²⁹M. G. Blaber, M. D. Arnold, and M. J. Ford, *J. Phys. Chem. C* **113**, 3041–3045 (2009).
- ³⁰J. B. Lassiter, J. Aizpurua, L. I. Hernandez, D. W. Brandl, I. Romero, S. Lal, J. H. Hafner, P. Nordlander, and N. J. Halas, *Nano Lett.* **8**, 1212–1218 (2008).